A Design Concept for Multiple Lunar Swingby Trajectories

Roby S. Wilson* and Kathleen C. Howell†
Purdue University, West Lafayette, IN 47907

Abstract

The objective of this work is the development of efficient techniques for the preliminary design of trajectories that encounter the Moon multiple times and must satisfy specific trajectory requirements, such as apogee placement. The general solution approach proceeds in three steps. In an initial patched conic analysis, a timing condition is employed to construct an arbitrary number of trajectory arcs, which are then connected at lunar encounters to initialize the approximation. Next, multi-conic methods are used to incorporate lunar and solar gravity effects. An optimization procedure is then employed to reduce the effective velocity discontinuities and produce a fully continuous multiple lunar swingby trajectory. Finally, a numerical differential corrections process results in an integrated trajectory that satisfies the constraints, and includes appropriate lunar and solar gravitational models.

Introduction

The goal of this study is the development of a design tool to create multiple lunar swingby trajectories in an efficient and accurate manner, that is applicable in a variety of mission scenarios. Many authors have contributed to the development of this trajectory concept, originating with Farquhar and Dunham in 1980.[1] In their concept, pairs of lunar swingbys are used to alternatively raise and lower the apogee distances, while advancing the line of apsides in such a way that the desired orbit orientation is maintained relative to the Sun-Earth line. A multiple lunar swingby (MLS) trajectory is defined here as a similar series of these double lunar swingby trajectories.

In this analysis, the problem solution is separated into a sequence of increasingly complex steps. Initially, the trajectory is approximated as a series of geocentric conic ars that encounter the Moon at the beginning and end of each leg. This two body analysis, as described in Howell and Marsh,[2] uses a massless Moon in an eccentric orbit about the Earth to solve for the desired "collision" arcs that meet the specified requirements. This conic analysis is useful in estabilishing general trajectory characteristics such as: orientation relative to the Sun, apogee distances, and approximate lunar encounter times. In the next step of the process, the patched conic approximation is improved to include lunar and solar gravity effects that were neglected in the conic design. In this step, multi-conic techniques are used to incorporate the effects of the additional gravity fields, with the goal of preserving the general characteristics designed using patched conics. In addition, a differential corrections process is employed to ensure position and velocity continuity along the path. In the final step, the results are numerically integrated using a Sun-Earth-Moon (SEM) model in which solar and lunar positions are determined from polynomial representations of ephemeris data. A differential corrections process is then used to ensure position and velocity continuity. This approach differs from the procedure suggested by Ishii and Matsuo[3] in that an intermediate step has been added to help maintain the desired orbital characteristics and to facilitate the numerical integration process. This work focuses primarily on the intermediate step between the patched conic analysis and numerical integration.

*Graduate Student, School of Aeronautics and Astronautics, Member AIAA, Member AAS

†Associate Professor, School of Aeronautics and Astronautics, Senior Member AIAA, Member AAS

Background

For the multiple encounter problem, we are interested in the identification of a specific solution for the motion of a spacecraft in the restricted three (or four) body problem. In particular, we will apply the methodology in the Sun-Earth-Moon system. Although it is possible to generalize this approach to other primary systems, the SEM system has been the focus of some recent mission planning and, thus, it is the system of choice for this study. To non-dimensionalize the problem, then, define the following characteristic quantities: $G \cdot M^* = 40353$ km^3/sec^2, $L^* = 388424$ km, and $T^* = 381097$ sec, corresponding to the mass of the Earth-Moon system, the average distance between the Earth and Moon, and characteristic time selected such that the non-dimensional gravitational parameter is unity.

Coordinate Systems

The analysis in this work is accomplished using three coordinate systems: Earth Inertial (EI), Moon Inertial (MI), and Solar Rotating (SR). The first two frames (EI and MI) are the principal working frames used in the problem analysis and are defined as follows. The Earth Inertial frame ($\hat{X}_e$, $\hat{Y}_e$, $\hat{Z}_e$) has its origin at the center of the Earth and is defined consistent with the mean ecliptic and equinox of 1950. The Moon Inertial frame

$(\hat{X}_m,\ \hat{Y}_m,\ \hat{Z}_m)$ has its origin at the center of the Moon and each axis remains parallel to the corresponding axis in the EI frame. The origin of the Solar Rotating frame $(\hat{x}_s,\ \hat{y}_s,\ \hat{z}_s)$ is located at the center of the Earth, with the $\hat{x}_s$ axis parallel to the vector from the Sun to the Earth. The $\hat{z}_s$ axis is coincident with $\hat{Z}_e$, and $\hat{y}_s$ lies in the ecliptic plane such that $\hat{y}_s$ equals $\hat{z}_s \times \hat{x}_s$.

Two Body Problem State Transition Matrices

The methodology in this work relies heavily upon the use of the state transition matrix (STM). To simplify notation, denot $[\Phi_{fi}] = [\Phi(t_f,\ t_i)]$ as the STM from time t_i to t_f. By using the state transition matrix, an error in the final state can be eliminated by appropriate changes in the initial state. This relationship is the foundation of the differential corrections procedures used in this work for targeting purposes.

A major advantage associated with the two body model is the availaibility of analytic expressions for the elements of the state transition matrix.[4] These partials are either elliptic or hyperbolic, corresponding to the conic reference orbit of ineterest. These expressions offer a quick method for determination of the state transition matrix that will be extremely useful in the second step of the solution process employing multi-conic techniques.

Patched Conic Analysis

In order to develop a multiple lunar swingby trajectory, an initial approximation issought that satisfies the specified design requirements. A quick and relatively straightforward method to determine this initial estimate is based on two solutions using patched conics.

Patched Conic Analysis (PCA) employs Earth-centered conics to create the desired trajectory, while neglecting the lunar and solar gravity effects. By specifying that each conic segment begin and end with a lunar encounter, an approximate MLS trajectory can be created simply by "patching" these geocentric conic segments together at consecutive lunar encounter points. Conic analysis does not model the lunar flyby and, in fact, since the lunar gravity is neglected, each lunear encounter is, in effect, a collision with the center of the Moon. This introduces errors into the solution that, in general, make it impossible to use the trajectories resulting from PCA to generate initial conditions that can be satisfactorily propagated numerically to produce a continuous path in the complete three (or four) body model. Despite these errors, PCA does yield a useful initial approximation to the solution, and provides a basis of comparison for the final iintegrated trajectory.

The motivation for incorporating multiple lunar swingbys into the trajectory may vary, but frequently the goal is to orient the spacecraft trajectory in a certain direction relative to the SR frame. The concept proposed by Farquhar and Dunham,[1] using lunar gravity assists to advance the line of apsides at the rate required to "fix" the orbit in the SR frame, is employed in the analysis to maintain the orientation of the spacecraft line of apsides parallel to the $\hat{x}_s$ axis. The theoretical basis for determining lunar encounters at appropriate time intervals lies in the development of a timing condition relating the motion of the Sun, Earth, Moon, and spacecraft.

The Timing Condition

To construct a multiple lunar encounter trajectory, a method is required to design a series of Earth-centered conic segments that begin and end with lunear encounters, and are oriented in the desired direction relative to the SR frame. This ensures that the spacecraft and the Moon will be in the same vicinity at the appropriate times. Hence, orbits are sought that collide twice with the Moon, thus identifying conic arcs that begin and end with lunar encounters. ¿From detailed discussions in Howell and Marsh,[2] Marsh and Howell,[5] and Marsh,[6] it is apparent that the determination of such conic arcs can be reduced to the solution of a single algebraic equation, called the Timing Condition (TC). The functional form of this timing condition, from Howell and Marsh,[2] is an implicit algebraic function of the form

$$TC(e_m,\ \phi,\ \sigma_i,\ n,\ m;\ a,\ e) = 0\ . \qquad (1)$$

The variable e_m represents the eccentricity of the lunar orbit about the Earth with perigee at P_m. (See Figure 1.) The angle ϕ, also shown in the figure, describes the orientation of the orbit line of apsides with respect to the lunar line of apsides, measured clockwise from the $\hat{X}$ axis. The σ_i parameters comprise a set of switching functions used to parameterize the Earth-centered orbit, as described in

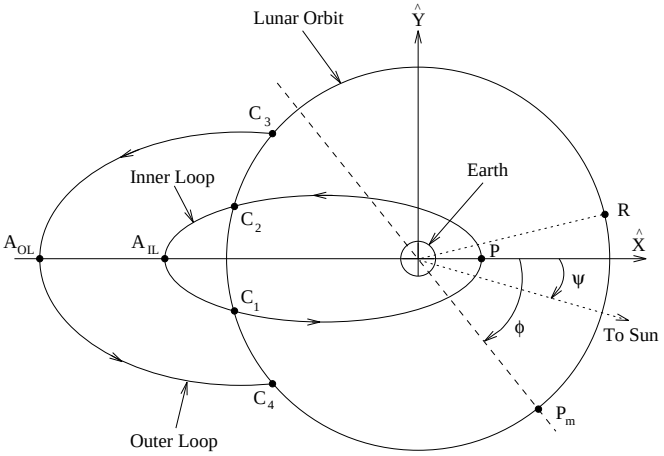

Fig. 1. Conic Arc Definitions

Howell and Marsh.[2] The integers n and m are used to identify unique solutions to the timing condition. They describe the numbers of non-encounter intersections of the Moon with the conic orbit (n), and non-encounter crossings of the spacecraft path with the lunar orbit (m).

The solution of this algebraic function yields two of the orbit parameters, a and e, associated with the conic segment, as well as the eccentric anomalies corresponding to the spacecraft and lunar locations in their respective orbits at the collision points. ¿From these values, the true anomalies corresponding to the positions of the spacecraft ($\theta_c - \omega_c$) and Moon ($\theta - \omega$) and the times of the lunar encounters can be determined at the beginning and end of the conic segment. These times are represented at t_c, and t_{cf}, corresponding to the initial and final times of the lunar encounters. Note that $t = 0$ is defined at a spacecraft crossing of the line of apsides (at perigee P, or apogee A_{OL} or A_{IL}) according to σ_2. (See Figure 1.) Therefore, by convention, t_c, will be less than zero and t_{cf} will be greater that zero. Furthermore, due to the near symmetry of the problem, the spacecraft, Earth, and Moon will be nearly collinear along the spacecraft line of apsides at $t = 0$. This configuration defines the conic inertial frame ($\hat{X}$, $\hat{Y}$), with the Moon at $t = 0$ (point R) determining the half plane containing the $+\hat{X}$ axis.

Conic Arc Selection

Once the conic arc has been determined from the solution of the timing condition, it is necessary to orient this segment in the SR frame with respect to the Sun-Earth line. It is assumed in the solution process that the conic orbit plane for each segment is coincident with the lunar orbit plane. Therefore, the conic orbit parameters Ω_c (ascending node) and i_c (inclination) are equal to those available for the lunar orbit. Thus, it is possible to completely define the appropriate conic segment, as well as its orientation, in terms of the lunar orbit. The segment is repesented by the orbit parameters (Ω_c, i_c, θ_c, a, e, t_c) at each endpoint.

After the conic orbit plane is quantified in terms of the lunar orbit plane, orientation of the spacecraft orbit is accomplished through identification of epochs corresponding to appropriate locations of the Sun and Moon relative to the Earth, and to each other. Such eposch result from an iterative search through data that represents solar and lunar ephemerides. This process is aided by te inherent near symmetry of consecutive collision orbits.[5] Since the Moon and the spacecraft must collide at the endpoints of the conic arc, they also tend to cross the spacecraft line of apsides at roughly the same time. If the epoch at which the spacecraft crosses its line of apsides is defined as time t_{aps}, then the Earth, Moon, and spacecraft will be nearly collinear along the $\hat{X}$ axis. Orientation relative to the Sun can thus be accomplished by constraining t_{aps} to occur at a time when the Sun, Earth, and Moon are positioned appropriately, through a search for solar-lunar conunctions and oppositions. The angle ψ (Figure 1) specifies the orientation of the spacecraft line of apsides with respect to the Sun-Earth line. This angle is ideally equal to 0° for a trajectory with anti-solar pointing apogees and equal to 180° for one with solar pointing apogees.

There are two types of sulutions for the conic arcs generated by this approach, as shown in Figure 1. The first type of conic arc is termed an "inner" loop,[6] and can be described as having at least one perigee and some number of apogees during the time from one lunar encounter to the next. The other type of conic segment is called an "outer" loop,[6] and is characterized by trajectories that pass through only one apogee and no perigees during the time from one lunar encounter to the next Given the starting requirements, the outer loops generally occur for even numbered segments in the MLS problem. The inner loops, then, occur for odd numbered segments, beginning with the insertion arc to initiate the multiple swingby trajectory, and serve as connecting segments between successive outer loops. To meet mission objectives, it is desirable to ensure that the outer loops are as closely oriented as possible with the desired direction in the SR frame.

For construction of a complete multiple lunar encounter path, series of conic arc segments must be propery sequenced using the conic arc segments must be patched together at lunar encounters. The arcs must be properly sequenced using the conic arc selection process to assure an orbit orientation history consistent with the requirements. The entire process of creating a multiple lunar encounter trajectory by patching these conic arc segments together is called Patched Conic Analysis (PCA).

Input Parameter Identification

The PCA process requires a set of input parameters that are determined from the design specifications for the mission. These parameters are used to solve for the orbital elemments describing the conic segments that make up the initial estimate of the slution to the MLS problem. The first input is the specification of the starting date for the initial lunar encounter in Julian format (JD_1). For the first segment, however, it is necessary to specify the injection date to initiate the trajectory. In order t facilitate a solution, this injection date is assumed to correspond to perigee on the first conic segment. To properly align the trajectory in the SR frame, the input date must actually correspond to the closest solar-lunar conjunction (for anti-sunward) or solar-lunar opposition (for sunward) prior to the desired injection date. The next inputs are the expected length of the conic segment in an integer number of months (N_{mos}) and the expected number of apogees (N_{apos}), Both of these values are estimates of the

general characteristics of the desired conic solution, and may be changed slightly by PCA to achieve the solution that best matches the specifications.

The fourth required input parameter is an estimate of the angle ψ. Since the majority of the flight time is spent in the outer loops, it is desirable for these segments to match this specification as closely as possible. For inner loops, however, it is often desirable from a mission design standpoint to specify the perigee passage distance (R_p) in addition to ψ. This usually results in some loss of control over the orientation angle ψ for the segment, but since the inner loops are generally shorter than the outer loops, this is not crucial to overall trajectory planning.

Given these inputs (JD_1, N_{mos}, N_{apos}, ψ, and possibly R_p) as desirable characteristics for the Earth-centered conics, the conic arc selection algorithm solves the timing condition iteratively, as described in Marsh,[6] for the properly oriented conic arc segments that best match the mission specifications. ¿From the solution to the TC, the bit parameters representing the conic arcs (Ω_c, i_c, θ_c, a, e) and the dates of the lunar encounters, JD_1 and JD_2, are obtained. all conic segments are then patched together at consecutive lunar encounters by PCA to create the two body approximation to the solution of the MLS problem.

Results from Patched Conic Analysis

A sample multiple lunar swingby trajectory, based on an example by Marsh,[6] has been designed using Patched Conic Analysis. The input and output parameters associated with each of the conic segments that result from the patched conic algorithm are shown in Table 1. The trajectory is comprised of four conic segments, two inner loops and two outer loops. This number of segments if arbitrary and the solution procedure is independent of the number of segments selected. For this trajectory, it was specified that the spacecraft apogees remain generally oriented in the anti-solar ($+\hat{x}_s$) direction, thus, $\psi = 0°$ was input for each of the four segments. An injection date equal to JD2449094.4 was specified for the first segment, corresponding to a conic orbit perigee on April 16, 1993. The first segment was estimated to last two months and contain four apogees. This required an input date corresponding to a solar-lunar conjunction on April 4, 1993 (JD2449082.3). In practice, this segment lasted about 15 days and contained one apogee, due to the fact that only one phasing orbit was actually retained to achieve the first lunar encounter on JD2449109.5 (May 2, 1993). A perigee distance (R_p) at the Earth of 12,000 km was specified for the first segment, but was achieved at the expense of a 20° rotation relative to the anti-solar direction in the SR frame. For all subsequent segments, propagation proceeded from the final state of the previous segment to the next lunar encounter. Segments 2 and 3 were designed to last one month each, with the third segment (the second inner loop) having a perigee passage distance equal to 52,000 km. The fourth and final segment was designed to last two months and was expected to be the largest segment of the trajectory, in terms of apogee distance. The conic arc elements a and e from the solution of the TC, as well as the actual trajectory duration are shown in Table 1 for each of the four segments in the trajectory. These results match those found in Marsh[6] and Spencer.[4]

Table 1. Input/Output Parameters for PCA

	Conic Segments			
Inputs	1	2	3	4
N_{mos}	2	1	1	2
N_{apos}	4	1	1	1
R_p (km)	1200	–	52000	–
ψ (deg)	0.0	0.0	0.0	0.0
Outputs	1	2	3	4
a (non-dim)	0.56937	1.30076	0.73197	1.88931
e	0.94574	0.79313	0.81710	0.80478
Δt (da)	27.1575	34.8901	24.3130	65.6179

When the resulting trajectory is projected onto the $x_s - y_s$ plane in the SR frame (Figure 2) it is seen that PCA generates a solution that maintains the outer loop apogees (denoted A_2 and A_4) in the anti-solar direction, as specified. Note that both outer loops, as well as the second inner loop, have their lines of apsides roughly alighned with the anti-solar direction, as desired, and provide coverage of the region between the Earth and the mean Sun-Earth L_2 point. Each of the lunar swingbys, or collisions in PCA, is denoted as S_i.

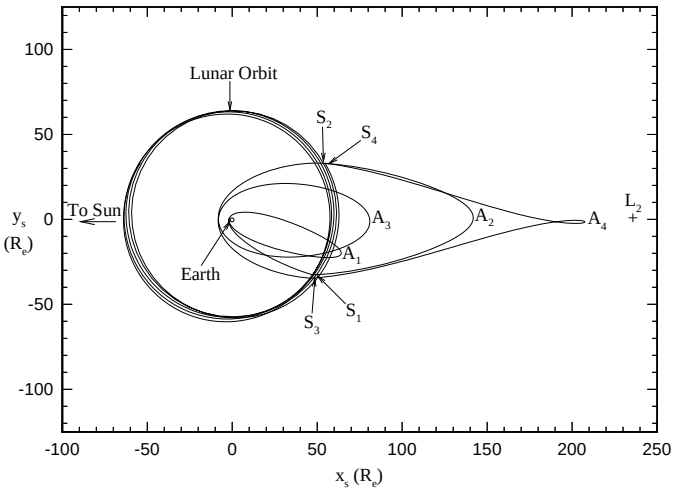

Fig. 2. PCA – $x_s y_s$ Projection in SR Frame

From the view of the trajectory in the SR frame, it is evident that PCA yields a good approximation to the solution of the MLS problem, with apogees aligned along the Sun-Earth line. Howver, by neglecting the lunar and solar gravity, errors are introduced into the solution. These errors are most evident in the large equivalent velocity discontinuities (approximately 1444.1 m/s total) at the lunar collision points. The poor modeling of the lunar encounters in PCA generally prevents the straightforward extension of the solution to produce a numerically integrated trajectory with the same design characteristics. Therefore, it becomes necessary to improve the conic results, so that a viable trajectory can be constructed.

Multi-Conic Analysis

As an intermediate step between PCA and numerical integration in the four body problem, a three body model with solar perturbations is employed to enable the conic result to serve as the basis for an improved solution to the MLS problem. The goal in this step is to employ the approximation techniques in a manner that will ultimately lead to a numerically integrated trajectory that retains the overall orbit characteristics designed using PCA.

The differential equations governing motion in the restricted three body problem are not, in general, solvable analytically. However, a number of authors have developed approximations that provide a reasonable representation of the spacecraft motion under various conditions. The solution approach used here was developed by Wilson[7] and Byrnes and Hooper,[8] among others, and is called multi-conic analysis.

When using multi-conics, the contributions of each primary to the motion of the spacecraft are evaluated separately as solutions to a two body problem, and then "overlapped" through the addition of a constant velocity segmen. The result is an approximation to motion in the restricted three body problem (R3BP), or the restricted four body problem (R4BP) if solar perturbations are included. Since a solution generated with multi-conics includes the gravitational effects of additional primaries, it should provide a more accurate method of representing the motion in the MLS problem.

State Transition Matrices Using Multi-Conics

Although, in general, no analytic solution is available for the STM in the R3BP or R4BP, the use of two body conics in the multi-conic approximations allows analytic representations for the elements of the STM to be developed from the two body STM's. The STM for a single multi-conic step may be determined by sequentially multiplying the STM's corresponding to each propagation step in the algorithm.

As an example, consider a spacecraft moving from the Earth to the Moon. The first step yields as STM from propagation of the Earth-centered conic, using the appropriate two body solution. This matrix relates the initial geocentric state to the final state of the Earth-centered (EC) conic, and is denoted Φ_{fi}^{EC}. Next, the final geocentric state is transformed to a selenocentric state, and the effects due to primary motion and solar perturbations are added. The transformation and effects of the primary motion do not effect the STM, however, the addition of the solar perturbation does contribute by changing the end state on the EC conic in some specified manner. The effective STM for this segment is denoted Φ_{ff}^{Sun}. In the field free segment (motion under no gravitational force fields), the state is propagated backwards along the selenocentric velocity vector to the initial time. The STM corresponding to the field free trajectory, Φ_{if}^{FF}, is simply a linear function of the propagation time $\Delta t = t_f - t_i$. In the final step of the algorithm, a Moon-cenetered conic is propagated forward in time to obtain the approximation to the final selenocentric state. This conic STM is denoted Φ_{fi}^{MC} and relates the initial state on the Moon-centered conic to the final selenocentric state. Because the multiconic trajectory is continuous, and since all the STM's are defined relative to the EI or MI coordinate frame, the determination of the complete STM that maps changes in the initial state of the multi-conic step to changes in the final state involves multiplying these four matrices sequentially to obatin

$$\left[\Phi_{fi}^{\mathrm{step}}\right] = \left[\Phi_{fi}^{\mathrm{MC}}\right]\left[\Phi_{if}^{\mathrm{FF}}\right]\left[\Phi_{ff}^{\mathrm{Sun}}\right]\left[\Phi_{fi}^{\mathrm{EC}}\right] \quad . \qquad (2)$$

A similar STM can be computed for each of the multiconic steps along a given path, and then sequentially multiplied to create the state transition matrix for the entire trajectory. This complete matrix associated with the multi-conic approximation of the trajectory is employed in various differential corrections procedures to target desired endstates for the MLS problem.

Pseudostate Theory

Application of the multi-conic technique, as described above, is very successful at approximating specific state vectors in the R3BP or R4BP. However, the algorithm becomes less effective if the trajectory includes a close passage of the second primary (in this case, the Moon). Since modeling of the lunar flybys is one of the primary reasons for using multi-conics in the analysis, a modified version of the multi-conic algorithm must be employed. This modified algorithm, developed by Wilson[7] in conjunction with the Byrnes and Hooper algorithm, is based on pseudostate theory. The basic approximations are the same as those associated with the previous multi-c0nic algorithm (without solar perturbations), but it effectively

models hyperbolic trajectories relative to the Moon.

A state transition matrix can be computed for the pseudostate approximation by sequentially multiplying the STM for each of the propagation steps in the pseudostate algorithm. This pseudostate STM is crucial in the determination of the lunar swingby through a solution of the three body Lambert problem (3BLP). Among various attemtps at approximating the solution of the three body Lambert problem, a particularly appropriate solution approach was proposed by Byrnes[9] using pseudostate theory and the resulting STM in a differential corrections process. This procedure forms the basis of the targeting scheme to identify a solution that passes through specified position states before and after the lunar flyby, or in other words, to bridge the "gaps" in the solution left by the poor modeling of the lunar encounter using PCA.

These specified states, called patch points, around the lunar flybys are determined in PCA and represent the boundary between the two types of multi-conic algorithms. The patch points are determined by terminating the conic area from PCA at a predetermined lunar sphere of influence. A value of 25 Earth radii has been found to yield a reasonable balance between accuracy and multi-conic efficiency. These patch point states are used to initialize the multi-conic procedures.

Multi-Conic Analysis (MCA)

To apply the multi-conic approximation to the MLS problem, it is necessary that a discrete set of states be available to start the algorithm. ¿From PCA, state vectors representing the $2k$ patch points are available for the k segments that comprise the PCA estimate of the MLS trajectory. Between the initial and final endstates associated with each segment, MCA is applied to generate an updated solutin for that segment.

To begin, the length of each multi-conic step in the algorithm is computed. The total flight time for the segment under consideration is divided by an integer value to obtain a multi-conic step size (Δt) of roughly 6 hours. It has been determined that a multi-conic step size of approximately 6 hours yields sufficient accuracy in the Sun-Earth-Moon problem without sacrificing computational speed. The first multi-conic step is propagated from the initial time t_i to the time $t_j = t_i + \Delta t$, and the state transition matrix, $\left[\Phi_{ji}^{\text{step}}\right]$, for this step is computed using the two body approximations. The endstate at the final time, t_j, then becomes the initial state for the next step, and the process is repeated until the final time for the entire trajectory segment is reached. The position state at the end of the final multi-conic step is compared to the desired final patch state for the segment. If the difference between the position states is greater than a specified tolerance, the complete STM for the segment is computed, and used to differentially correct the velocity state at the initial point on the segment to reduce the error. Note that in the differential corrections process, the initial position state and time are constrained to remain unchanged from the PCA solution. This entire process is repeated until the final position state from MCA is within the prescribed tolerance. This algorithm is repeated for each of the segments along the MLS trajectory.

In practice, it was found that the jump from PCA to MCA including the solar perturbations was too great for the differential corrections process. So initially, MCA is applied to the PCA results using only the lunar gravity. After an acceptable convergence has been achieved, the solar perturbations are added (see Byrnes and Hopper[8]) and the four body approximation is obtained.

Pseudostate Analysis (PSA)

After MCA is applied to the segments from PCA and the states at the patch points have been updated, it is then necessary to model the lunar flybys to create a trajectory that is continuous in position, as well as time. Pseudostate Analysis (PSA) is used between the boundary states at the beginning and end of consecutive MCA segments to model the lunar flybys.

For use as input to PSA, the updated states at the patch points are available from the MCA solution. PSA is employed to determine a trajectory arc that will bridge the gap between one segment and the next, that is, model the lunar swingby. So, the final state of one segment and the initial state of the next define the target points for PSA (termed *swingby states*). Between the initial and final swingby states, a two body Lambert problem (relative to the Moon) is solved to yield an estimate of the lunar peripsis state and th time of closest approach. The 2BLP solution with the smallest velocity discontinuity at the patch points is used t ensure proper lunar passage.

After the initial estimate of the perilune state is computed, the lunar swingby is approximated by application of the Byrnes pseudostate procedure[9] to produce a trajectory arc between the initial and final swingby states. This yields an estimate of the perilune state, as well as a second estimate of the velocity states at the swingby points.

At this stage, the trajectory has position continuity at the MCA/PSA patch points. However, velocity discontinuities may now be present at each patch point. The current esimate of the outgoing velocity state from PSA is compared with the incoming velocity state estimate from MCA to compute the patch point $\Delta\bar{V}$'s, that is,

$$\Delta\bar{V} = \bar{V}^{+} - \bar{V}^{-} \ , \tag{3}$$

where overbars indicate vectors. Ntoe that for an initial swingnby point, superscript + denotes the velocity from PSA and - denotes the velocity from MCA, and vice verse

for a final swingby point. These patch point $\Delta\bar{V}$'s are computed in Earth Inertial coordinates. The reduction of these velocity discontinuities is the next step.

Results

The improved trajectory from MCA/PSA is viewed in the SR frame as a projection onto the $x_s - y_s$ plane (Figure 3). The trajectory includes all of the propagation steps that comprise the MCA and PSA procedures. The "spikes" seen in the plot represent the various propagation steps, and are not representative of the "true" path. Although the MCA/PSA solution actually consists of a set of discrete solution states, plotting all of the various steps in the MCA/PSA algorithms shows the general characteristics of the trajectory quite well.

Notice that the general trajectory shape from PCA has been preserved and the apogee characteristics have been maintained. A significant difference between the two approximate trajectories in Figure 2 and 3 concerns the region near the three swingbys. Although both solutions are continuous in position, the single velocity ciscontinuities at the lunar collision points in PCA are now replaced by velocity discontinuities at the two patch points in MCA/PSA. Recall that initially the total equivalent velocity discontinuity in the PCA solution was 1334.1 m/s. After including the four body effects, this total is reduced to 773.9 m/s using MCA/PSA. Although this is still not acceptable, the improvement is obvious.

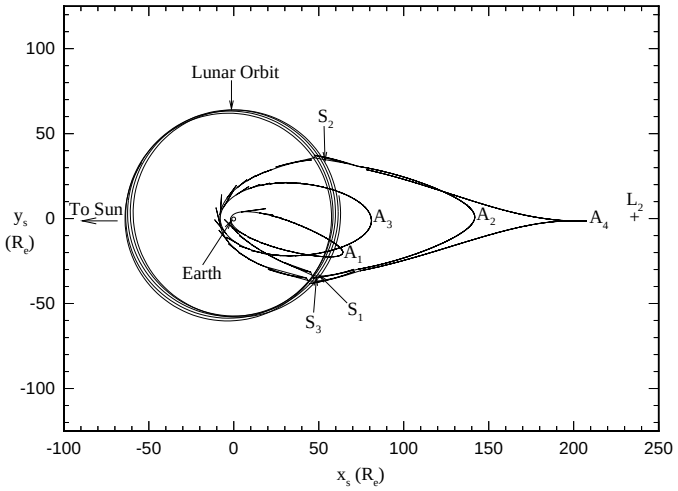

Fig. 3. Initial MCA/PSA – $x_s y_s$ Projection – SEM

Reduction of Velocity Discontinuities

The ultimate goal in the second step of the solution process is a multiple lunar swingby trajectory that meets the design specifications and is continuous in both position and velocity, as well as time. Thus, it is desired to create an automated process to simultaneously reduce the patch point velocity discontinuities throughout the solution. This is accomplished by varying the patch point states and times in a specified manner using a differential corrections scheme. The resulting patch point $\Delta\bar{V}$'s can be reduced significantly, if not eliminated altogether, while the general characteristics of the PCA solution are retained, so that the numerically integrated trajectory accurately reflects the design specifications.

The "costs" associated with the multi-conic estimate is defined as the sum of the magnitudes of all the velocity discontinuities along the trajectory. Define, then, a velocity discontinuity vector $\Delta\bar{V}_{ij}$ in Earth Inertial coordinates at each of the patch points consistent with Equation (3), where the subscript i denotes the swingby number (1, 2 or 3) and j identifies the swingby patch point, either (1) prior to periapsis passage, or (2) post-passage. In addition, let $\bar{V}_s$ denote the initial velocity for the complete trajectory and $\bar{V}_f$ be the velocity state at the completion of the nominal trajectory. (Note that no velocity discontinuities exist at these points.) The patch point states themselves are also expressed using the ij subscript convention. Defined as such, the total cost (ΔV_{tot}) for a given trajectory is the sum of all $|\Delta\bar{V}_{ij}|$ in the solution. This cost must be minimized while retaining the trajectory characteristics designed using PCA.

Derivation of the State Relationship Matrix

To employ a differential corrections process to reduce the total cost, it is necessary to derive the relationships between a given patch point $\Delta\bar{V}_{ij}$ and the independent variables in the problem. Since the multiple lunar swingby trajectory is described in terms of $2k$ discrete states and times as the independent parameters. It has been determined that including the apogee states as additional independent parameters adds flexibility, improves the convergence of the solution, and produces solutions that better reflect the original PCA result. Therefore, it is necesssary to determine the variation of each $\Delta\bar{V}_{ij}$ due to variations in the patch point positions and times and apogee positions and times, which until now have been fixed at values determined during PCA. A linear relationship between these states can be represented in matrix form as

$$\left\{ \begin{array}{c} \delta\Delta\bar{V}_{ij} \\ \delta\Delta\bar{V}_{A_k} \end{array} \right\} = [M] \left\{ \begin{array}{c} \delta\bar{R}_{ij} \\ \delta\bar{R}_{A_k} \\ \delta t_{ij} \\ \delta t_{A_k} \end{array} \right\} , \qquad (4)$$

where

$$[M] = \left[\begin{array}{cc|cc} \frac{\partial\Delta\bar{V}_{ij}}{\partial R_{ij}} & \frac{\partial\Delta\bar{V}_{ij}}{\partial R_{A_k}} & \frac{\partial\Delta\bar{V}_{ij}}{\partial t_{ij}} & \frac{\partial\Delta\bar{V}_{ij}}{\partial t_{A_k}} \\ \frac{\partial\Delta\bar{V}_{A_k}}{\partial R_{ij}} & \frac{\partial\Delta\bar{V}_{A_k}}{\partial R_{A_k}} & \frac{\partial\Delta\bar{V}_{A_k}}{\partial t_{ij}} & \frac{\partial\Delta\bar{V}_{A_k}}{\partial t_{A_k}} \end{array} \right] . \qquad (5)$$

and A_k denotes the k^{th} apogee state. Notice that the $m \times n$ matrix $[M]$ in this relationship (called the State Relationship matrix or SRM) is not square. In the current example with three swingbys, there are 30 dependent scalar variables (3 for each $\Delta\bar{V}_{ij}$ and $\Delta\bar{V}_{A_k}$ at the apogee states) and 48 independent parameters ($\bar{R}_{ij}$ and t_{ij} - including $\bar{R}_s$, t_s and $\bar{R}_f$, t_f, as well as $\bar{R}_{A_k}$ and t_{A_k}). Since this system is underdetermined, there are infinitely many solutions. It is therefore possible to estimate the changes in the values of the independent variables that are necessary to reduce the $\Delta\bar{V}_{ij}$, and thus, the total cost. Although the size of the matrix is large, this disadvatage is offset by the fact that the STM's from MCA/PSA can be used to produce expressions for each of the partials in the matrix.[10]

Variations with Positions

To determine analytic expressions for the elements in the SRM, begin by examining, in general, the relationship between the variations of $\Delta\bar{V}_{ij}$ at some point N and changes in the independent position parameters. Split $\Delta\bar{V}_N$ into its component parts, as in Equation (3), and take the partial derivative with respect to the preceding position state $\bar{R}_{Nf-1}$. The expression in the SRM becomes

$$\frac{\partial \Delta\bar{V}_N}{\partial \bar{R}_{N-1}} = \frac{\partial \bar{V}_N^+}{\partial \bar{R}_{N-1}} - \frac{\partial \bar{V}_N^-}{\partial \bar{R}_{N-1}} \ , \qquad (6)$$

where superscript + and - denote incoming or outgoing velocities according to Equation (3). Now, consider a change in starting position, $\delta\bar{R}_{N-1}$, and the impact of such a variation on the velocities along the trajectory arc fromthe 3BLP solution connecting states $N-1$ and N; all other independent variables are treated as constant.

¿From the three patch point position vectors $\bar{R}_{N-1}$, $\bar{R}_N$, and $\bar{R}_{N+1}$, and the respective times t_{N-1}, t_N, and t_{N+1}, identify two trajectory arcs, one from point N to point $N+1$. The two trajectory segments are each solutions of a three body Lambert problem. Since state transition matrices corresponding to these solutions are available from MCA/PSA, the Lambert partials described in D'Amario et al.[11] can be used to evaluate the partials in Equation (6).

First, consider the partial $\frac{\partial \bar{V}_N^-}{\partial \bar{R}_{N-1}}$ in Equation (6). The changes in the final position and velocity states at the end of the first 3BLP segment can be written as a function of the changes in the initial state through the known state transition marix $[\Phi_{NN-1}]$, that is

$$\left\{ \begin{array}{c} \delta\bar{R}_N \\ \delta\bar{V}_n^- \end{array} \right\} = [\Phi_{NN-1}] \left\{ \begin{array}{c} \delta\bar{R}_{N-1} \\ \delta\bar{V}_{N-1}^+ \end{array} \right\} \ , \qquad (7)$$

$$= \left[\begin{array}{cc} A_{NN-1} & B_{NN-1} \\ C_{NN-1} & D_{NN-1} \end{array} \right] \left\{ \begin{array}{c} \delta\bar{R}_{N-1} \\ \delta\bar{V}_{N-1}^+ \end{array} \right\} \qquad (8)$$

where $i = N$ and $j = N-1$. The matrices A_{NN-1}, B_{NN-1}, C_{NN-1}, and D_{NN-1} represent the four 3×3 submatrices $\frac{\partial \bar{R}_N}{\partial \bar{R}_{N-1}}$, $\frac{\partial \bar{R}_N}{\partial \bar{V}_{N-1}^+}$, $\frac{\partial \bar{V}_N^-}{\partial \bar{R}_{N-1}}$, and $\frac{\partial \bar{V}_N^-}{\partial \bar{V}_{N-1}^-}$, respectively. To determine the change in the final velocity ($\delta\bar{V}_N-$) on this first segment for a given change in the position at $N-1$, fix the final position at state N, as well as the initial and final times t_{N-1} adn t_N, and evaluate Equation (7) to produce the two relationships

$$\bar{0} = A_{NN-1}\delta\bar{R}_{N-1} + B_{NN-1}\delta\bar{V}_{N-1}^+ \ , \qquad (9)$$

$$\delta\bar{V}_N^- = C_{NN-1}\delta\bar{R}_{N-1} + D_{NN-1}\delta\bar{V}_{N-1}^+ \ , \qquad (10)$$

When rearranged, these yield expressions for the Lambert partials that reflect the sensitivity of the initial and final velocities on the segment to changes in the iniial position, that is,

$$\frac{\partial \bar{V}_{N-1}^+}{\partial \bar{R}_{N-1}} = -B_{NN-1}^{-1}A_{NN-1} \ , \qquad (11)$$

$$\frac{\partial \bar{V}_N^-}{\partial \bar{R}_{N-1}} = -D_{NN-1}B_{NN-1}^{-1}A_{NN-1} \ , \qquad (12)$$

Next, consicer the partial $\frac{\partial \bar{V}_N^-}{\partial \bar{R}_{N-1}}$ in Equation (6). Since the segment from $N-1$ to N is a solution to a 3BLP, $\bar{V}_N^+$ only depends upon the initial and final positions associated with the segment and the time of flight. However, since it was assumed that the changes in all independent variables in Equations (10) and (11), the positions and times associated with the patch points N and $N+1$ must also be constrained to be constant, thus, $\delta\bar{R}_N = \delta\bar{R}_{N+!} = \bar{0}$, and $\delta t_N = \delta t_{N+1} = 0$, hence

$$\frac{\partial \bar{V}_N^+}{\partial \bar{R}_{N-1}} = [0] \ . \qquad (13)$$

Combining Equations (11) and (12) into (6) produces

$$\frac{\partial \Delta\bar{V}_N}{\partial \bar{R}_{N-1}} = -C_{NN-1} + D_{NN-1}B_{NN-1}^{+}A_{NN-1} \ . \qquad (14)$$

Through a similar process, it can be shwon that the variations of $\Delta\bar{V}_N$ with the positions $\bar{R}_N$ and $\bar{R}_{N+1}$ are

$$\frac{\partial \Delta\bar{V}_N}{\partial \bar{R}_N} = -B_{N+1N}^{-1}A_{N+1N} - D_{NN-1}B_{NN-1}^{-1} \qquad (15)$$

$$\frac{\partial \Delta\bar{V}_N}{\partial \bar{R}_{N+1}} = B_{N+1N}^{-1} \ . \qquad (16)$$

The partials of $\Delta\bar{V}_N$ with respect to al other patch point positions can be shown to be zero by arguments similar to those above; namely, that the change in $\bar{R}_{N-1}$ does not affect $\bar{V}_N^+$, or that the change in $\bar{R}_{N+1}$ does not affect $\bar{V}_N^-$. The expressions in Equations (13)-(15) are evaluated from the STM's determined during MCA/PSA, and are used to form the columns of the matrix in Equation (5) relating the $\Delta\bar{V}_{ij}$ at the patch points to chanes in the patch point and apogee position states.

Variation with Times

Variation of the times associated with the patch point and apogee states is also an option. It is thus necessary to determine the partial derivatives of the $\Delta\bar{V}_{ij}$ with respect to the times associated with each patch point stae. This is accomplished through a process similar to the one used to determine the partials with respect to the patch point positions. Now, however, it is necessary to include the effect of a differential change in time in the expression for the state differentials.

First, note that the change in state due to a differential change in time, δt, can be estimated by a first order approximation as,

$$\delta\bar{R}(t+\delta t) = \delta\bar{R}(t) + \bar{V}\delta t \ , \quad (17)$$

$$\delta\bar{V}(t+\delta t) = \delta\bar{V}(t) + \bar{a}(t)\delta t \ , \quad (18)$$

where $\bar{a}$ is the acceleration of the spacecraft at the given instant, t.

Returning again to the matrix in Equation (5), we can write the expression relating the change in $\Delta\bar{V}_N$ to the change in time t_{N-1} as

$$\frac{\partial\Delta\bar{V}_N}{\partial t_{N-1}} = \frac{\partial\bar{V}_N^+}{\partial t_{N-1}} - \frac{\partial\bar{V}_N^-}{\partial t_{N-1}} \ , \quad (19)$$

The second partial in this expression can be determined in the same manner as before. Substituting Equations (16) and (17) for the changes in the initial position and velocity state, and using the STM from state N to state $N-1$ to replace $\delta\bar{R}_{N-1}(t_{N-1})$ and $\delta\bar{V}_{N-1}^+(t_{N-1})$ by a corresponding expression in terms of $\delta\bar{R}_N(t_N)$ and $\delta\bar{V}_N^1$), we can rewrite the two equations in the form,

$$\left\{ \begin{array}{c} \delta\bar{R}_{N-1}(t_{N-1}+\delta t_{N-1}) \\ \delta\bar{V}_{N-1}^+(t_{N-1}+\delta t_{N-1}) \end{array} \right\} = \left\{ \begin{array}{c} \delta\bar{R}_N(t_N) \\ \delta\bar{V}_N^-(t_N) \end{array} \right\} + \left\{ \begin{array}{c} \bar{V}_{N-1}^+(t_{N-1}) \\ \bar{a}_{N-1}^+(t_{N-1}) \end{array} \right\} \delta t_{N-1} \quad (20)$$

To detemine thepartial with respect to time t_{N-1}, we now constrain the initial and final differential positions on the segment, as well as the differential representing the change in the final time, tc be zero; thus only δt_{N-1} is non-zero. Incorporating these constraints and evaluating Equation (19) in the limit produces.

$$\frac{\partial\bar{V}_{N-1}^+}{\partial t_{N-1}} = \bar{a}_{N-1}^+ - D_{N-1N}B_{N-1N}^{-1}\bar{V}_{N-1}^+ \ , \quad (21)$$

$$\frac{\partial\bar{V}_N^-}{\partial t_{N-1}} = -B_{N-1N}^{-1}\bar{V}_{N-1}^+ \ . \quad (22)$$

Consistent with the procedure for the position differentials, the pseudostate partial of $\bar{V}_N^+$ with respect to t_{N-1} is zsero. Thus, Equation (18) becomes

$$\frac{\partial\Delta\bar{V}_N}{\partial t_{N-1}} = B_{N-1N}^{-1}\bar{V}_{N-1}^+ \ . \quad (23)$$

Similarly, it can be shown that the partials of $\Delta\bar{V}_N$ with respect to the times t_N and t_{N+1} are

$$\frac{\partial\Delta\bar{V}_N}{\partial t_N} = -D_{NN+1}B_{NN+1}^{-1}\bar{V}_N^+ + D_{NN-1}B_{NN-1}^{-1}\bar{V}_N^- \ , \quad (24)$$

$$\frac{\partial\Delta\bar{V}_N}{\partial t_{N+1}} = -B_{N+1N}^{-1}\bar{V}_{N+1}^- \ . \quad (25)$$

Note thatboth the multi-conic and pseudostate analyses employ the same approximations to the three body model, so the expressions for the accelerations cancel.

The partials of $\Delta\bar{V}_N$ with respect to the other patch point times are all zero, by arguments similar to those used in the derivation of Equation (12). The expressions in Equations (22)-(24) are evaluated from the STM's defined in MCA/PSA, and from the velocity states at the patch points. These elements comprise the columns of the right half of the matrix in Equation (5) relating the $\Delta\bar{V}_{ij}$ to the patch point times.

Reduction Algorithm

The $\Delta\bar{V}_{ij}$ reduction algorithm begins with the input of the patch point states and times, as well as apogee states and times, from the MCA/PSA solution, or directly from the PCA solution. For each long trajectory segment between flybys, Mca is applied between the initial patch point state the the apogee state, and then between the new apogee state and the final patch point state. The updated patch point states are then employed by PSA to generate a second estimate of the velocity states at the swingby points surrounding the flybys. The patch point $\Delta\bar{V}_{ij}$ and any apogee $\Delta\bar{V}_{A_k}$ are computed and the total cost ΔV_{tot} is checked against a desired tolerance. In the unconstrained case, as in our example, ΔV_{tot} is forced to a specified level (zero). However, if there are constraints placed on the target points, such as restrictions on the movement of the apogee states, then it may not be possible to reach the specified value, and a minimum solution is sought. In either case, the SRM in EQuation (5) is used in a differential corrections process to compute changes in the independent variables (positions and times) in an attempt to simultaneously reduce all the velocity discontinuities in the trajectory.

As noted, the SRM in Equation (5) is not invertible, and the system is underdetermined. Out of all possible solutions, choose the one with the smallest Euclidean norm, that is,

$$\left\{ \begin{array}{c} \delta\bar{R}_{ij} \\ \delta\bar{R}_{A_k} \\ \delta t_{ij} \\ \delta t_{A_k} \end{array} \right\} = [M]^T \left([M][M]^T\right)^{-1} \left\{ \begin{array}{c} \delta\Delta\bar{V}_{ij} \\ \delta\Delta\bar{V}_{A_k} \end{array} \right\} \ . \quad (26)$$

The differential changes computed in Equation (25) are added to the patch point and apogee states and then the

adjusted states are used to recompute an estimate of the trajectory w ith a ΔV_{tot} that is lower than that of the previous solution. This process is repeated until the specified value of ΔV_{tot} is achieved, or the change between succesive iterations is less than some specified tolerance. The final trajectory approximated from MCA/PSA is continuous in both position and velocity, or has a minimized ΔV_{tot}. The results are then input to a numerical propagation routine to achieve the final desired trajectory.

Results

The changes in position and velocity states, as well as times, between PCA and MCA/PSA after final application of the $\Delta\bar{V}$ reduction algorithm are shown in Table 2 for the example case. All times are reported in minutes, all position information is in km, and all velocity information is in m/s. Notice that each patch point has undergone significant alteration in terms of position and velocity, as well as time, relative to the PCA solution. The large changes made to the patch point and apogee states by the minimization algorithm further underscores the fact that, although PCA is useful as an initial estimate and as a design tool, a more accurate model is needed to fully integrate the effects of the Sun and Moon on the spacecraft's motion, and to create a fully continuous trajectory. Recall that the initial PCA solution had a total equivalent velocity discontinuity of 1334.1 m/s, which the MCA/PSA solution with solar perturbations lowered to 773.9 m/s. This cost has now been reduced to a total that is less than 1 m/s for the entire trajectory.

For completeness, Table 3 contains the elements, in dimensional MI coordinates, of the perilune state vector for each of the three flybys. Notice that each perilune passage (r_p) is well above the lunar surface, thus allowing for further modifications if necessary. The final times (in Julian format) associated with the lunar periapsis states are shifted ahead of the original collision dates from the PCA solution, and the periapsis state is altered by the algorithm to account for the timing errors introduced by PCA.

The trajectory is again plotted in the SR frame and shown in Figure 4. Comparison of the solution with the original trajectory generated from the PCA solution (Figure 2), or with the MCA/PSA solution (Figure 3), reveals the similarities between the solutions. Although there are noticeable changes in the trajectory from the corresponding PCA solution, the overall characteristics designed using the design process depends somewhat on the specifications, however, the near elimination of the velocity discontinuities testifies to the utility of this approximation and the value of the multi-conic techniques. It is expected, though, that some velocity discontinuity will be reintroduced when the results are numerically integrated.

Table 2. Changes in Patch Point and Apogee States

ΔJD_i	20.08	61.85	-362.85	136.85
ΔX_i	-1037.15	2248.66	6928.18	927.97
ΔY_i	-415.73	28071.19	60286.31	30462.27
ΔZ_i	-185.23	-3067.27	840.53	289.82
$\Delta \dot{X}_i$	402.71	13.34	-83.54	-50.51
$\Delta \dot{Y}_i$	251.73	37.59	408.51	25.99
$\Delta \dot{Z}_i$	-350.07	-19.62	-30.25	1.65
ΔJD_a	5.46	16.32	-4.56	-29.37
ΔX_a	-1678.01	30040.97	-15481.15	1589.55
ΔY_a	7314.75	37126.01	-34587.25	123913.30
ΔZ_a	4815.12	-13010.24	2493.41	-944.27
$\Delta \dot{X}_a$	-21.46	5.58	-51.18	20.69
$\Delta \dot{Y}_a$	4.80	-6.60	33.05	3.65
$\Delta \dot{Z}_a$	8.97	2.53	-1.46	-5.46
ΔJD_f	76.07	-111.0	370.44	47.33
ΔX_f	22755.09	26179l.26	55398.25	19962.30
ΔY_f	2547.46	16142.42	29062.16	-8340.21
ΔZ_f	579.74	2229.39	2874.03	-26351.43
$\Delta \dot{X}_f$	-92.15	.70	-446.20	-2.68
$\Delta \dot{Y}_f$	70.17	29.58	-152.69	-104.24
$\Delta \dot{Z}_f$	6.49	17.59	-31.64	7.69

Integrated Results

As a final step, it is necessary to demonstrate that the resulting multi-conic approximation has produced position and velocity states that can be successfully integrated to produce a viable estimate of the complete trajectory. The model for numerical integration includes the restricted four body equations of motion for the Sun-Earth-Moon system. In addition, the differential equations governing the STM are also numerically integrated to allow differential corrections processes to be employed on the integrated trajectory.

In order to numerically integrate the complete trajec-

Table 3. Final PSA Perilune States (in MI)

JD_p	2449109.50	2449144.12	2449169.01
x_p	12441.83	31772.78	-4573.77
y_p	8362.48	8879.90	26170.75
z_p	1911.73	5095.40	-1221.66
z_p	15057.85	33381.51	16595.48
$\dot{x}_p$	-698.58	-308.20	-1137.75
$\dot{y}_p$	1072.72	1130.42	-202.72
$\dot{z}_p$	-90.37	-48.19	-83.09

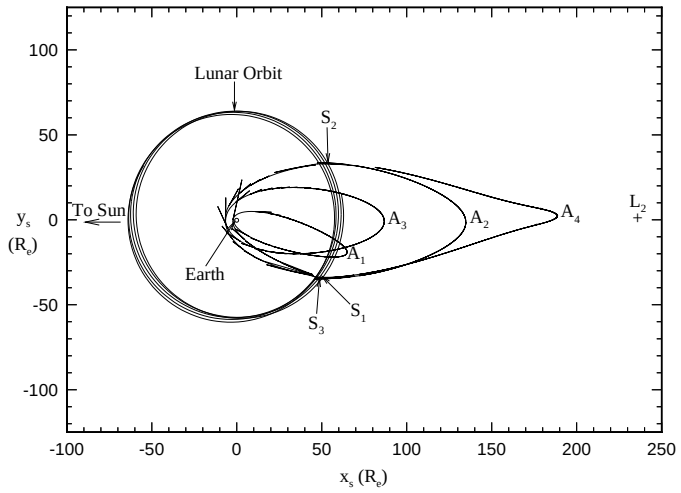

Fig. 4. Adjusted MCA/PSA – $x_s y_s$ Projeciton – SEM

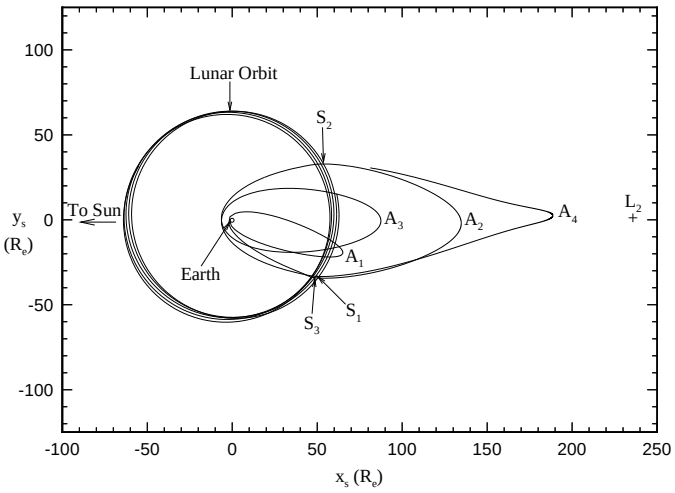

Fig. 5. Integrated – $x_s y_s$ Projection – SEM

tory, the $3k$ target states (patch point plus apogee states) from the reduction algorithm are again used to characterize the MLS trajectory. Between successive target states, a numerically integrated trajectory is propagated. Since MSA/PSA only approximates the R4BP, the numerically computed STM must be used to differentially correct the initial velocity associated with each segment to target the final position state along that segment, so that the path is again continuous in position. Unfortunately, because of this differential corrections prcoess, and due to the errors remaining the multi-conic approximations, velocity discontinuities reoccur at the target states along the integrated trajectory. Using an optimization process with a numerical SRM similar to that employed for the MCA/PSA results, the integrated trajectory can again be made continuous in velociy.

The numerical propagation process to generate the solutions employs the ISML library function DIVPRK, which is based on fifth-sixth order Runge-Kutta numerical integration scheme. All simulations are performed using double precision XL FORTRAN 2.3, with an integraion tolerance set to 5×10^{-15} in nondimensional units; all results are generated on an IBM RS-6000 model 580 running AIX 3.2.4.

Due to application of the numerical propagation process in this manner, velocity discontinuities arise again at each of the target points. The initial cost (ΔV_{tot}) associated with the integrated trajectory is approximately 39.7 m/s. Application of the SRM reduction scheme reduces this cost to 0.0 m/s in the unconstrained case.

The results are shown graphically in Figure 5 as a projection in the $x_s - y_s$ plan. Comparisons can easily be made to the corresponding trajectory approximations from PCA (Figure 2), initial MCA/PSA (Figure 3), and MCA/PSA afater the SRM reduction process (Figure 4). No large visible differences between the integrated results and the solutions that are continuous in velocity appear in any of the four segments. Thus, a fully continuous integrated trajectory is obtained that maintains the desired characteristics designed using PCA.

Conclusions

In summary, using Patched Conic Analyss and the solution to the Timing Condition, it is possible to generate MLS trajectories that meet the given design requirements. However, PCA introduces errors into the solution due to its failure to adequately model and incorporate the solar and lunar gravity.

Using MCA/PSA, it is possible to improve the PCA solution, while maintaining the desired design characteristics. The State Relationship Matrix, relating the velocity discontinuities in the solution to the patch point and apogee positions and times, is then employed to vary the positions and times of these states in a specified manner to simultaneously reduce all of the velocity discontinuities present in the trajectory. The resulting solutions retain the general characteristics designed using PCA, and are fully continuous in position, velocity, and time.

Representative states from these fully continuous trajectories are then introduced into a numerical propagation process based on the restricted four body model to produce a complete MLS trajectory. The trajectories obtained through this process are acceptable as solutions that meet the design criteria, but again, velocity discontinuities appear as a result of the trajectory construction process. A numerical optimization process similar to the one used on the MCA/PSA solution is then used to reduce this cost for the numerically integrated trajectory.

It is concluded, then, that use of the three step design

process results in an accurate, efficient method of constructing multiple lunar swingby trajectories that meet the design specifications for the problem. Furthermore, it is hoped that this procedure will prove useful in the determination of other types of solutions in the Sun-Earth-Moon system.

Acknowlegments

The authors would like to thank Purdue Unviersity for providing continuing support for this project. In addition, the efforst of Steven Marsh and David Spencer, who have contributed much to this work, are greatly appreciated.

References

[1]R. W. Farquhar and D. W. Dunham, "A New Trajectory Concept for Exploring the Earth's Geomagnetic Tail," *Journal of Guidance and Control*, Vol. 4, March-April 1981, pp. 192-196.

[2]K. C. Howell and S. M. Marsh, "A General Timing Condition for Consecutive Collision Orbits in the Limiting Case $\mu = 0$ of the Elliptic Restricted Problem," *Celestial Mechanics* Vol. 52, 1001, pp. 167-194.

[3]N. Ishii and H. Matsuo, "Design Procedue of Accurate Orbits in a Multi-Body Frame with a Multiple Swingby," *AAS Paper 93-655*, AAS/AIAA Astrodynamics Specialist Conference, Victoria, B.C., Canada, August 1993.

[4]D. A. Spencer, "Multiple Lunar Encounter Trajectory Design Using a Multi-Conic Approach," M.S. Thesis, Purdue University, December 1991.

[5]S. M. Marsh and K. C. Howell, "Double Lunar Swingby Trajectory Design," *Proceedings ofthe AIAA/AAS Astrodynamics Conference*, Minneapolis, Minnesota, August 1988, pp. 554-562.

[6]S. M. March, "Sun-Synchronous Trajectory Design Using Consecutive Lunar Gravity Assists," M.S. Thesis, Purdue University, May 1988.

[7]S. W. Wilson, "A Pseudostate Theory for the Approximation for Three-Body Trajectories," *AIAA Paper 70-1061*, AAS/AIAA Astrodynamics Conference, Santa Barbara, California, August 1970.

[8]D. V. Byrnes and H. L. Hopper, "Multi-Conic: A Fast and Accurate Method of Computing Space Flight Trajectories," —em AIAA Paper 70-1062, AAS/AIAA Astrodynamics Conference, Santa Barbara, California, August 1970.

[9]D. V. Byrnes, "Application of the Pseudostate Theory to the Three-Body Lambert Problem," *Journal of the Astronautical Sciences* Vol. 37, July-September 1989, pp. 221-232.

[10]R. S. Wilson, "A Design Tool for Constructing Multiple Lunar Swingby Trajectories," M.S. Thesis, Purdue University, December 1993.

[11]L. A. D'Amario, D. V. Byrnes, L. L. Scakett, and R. H. Stanford, "Optimization of Multiple Flyby Trajectories," *AAS Paper 79-162*, AAS/AIAA Astrodynamics Conference, Provincetown, Massachusetts, June 1979.